Supplementary data

Competition between bridged dinucleotides and activated mononucleotides determines the error frequency of nonenzymatic RNA primer extension

Daniel Duzdevich[1,2]*, Christopher E. Carr[1,3,4], Dian Ding[1,5], Stephanie J. Zhang[1,5], Travis S. Walton[1,6], and Jack W. Szostak[1,2,5,7]

[1] Department of Molecular Biology, Center for Computational and Integrative Biology, Massachusetts General Hospital, Boston, MA 02114, United States of America
[2] Howard Hughes Medical Institute, Massachusetts General Hospital, Boston, MA 02114, United States of America
[3] Department of Earth, Atmospheric and Planetary Sciences, Massachusetts Institute of Technology, Cambridge, MA, 02139, United States of America
[4] Current Address: Daniel Guggenheim School of Aerospace Engineering, School of Earth and Atmospheric Sciences, Georgia Institute of Technology, Atlanta, GA 30332, United States of America
[5] Department of Chemistry and Chemical Biology, Harvard University, Cambridge, MA 02138, United States of America
[6] Current Address: Department of Biological Chemistry and Molecular Pharmacology, Harvard Medical School, Boston, MA 02115, United States of America
[7] Department of Genetics, Harvard Medical School, Boston, MA 02115, United States of America

* To whom correspondence should be addressed. Email: duzdevich@molbio.mgh.harvard.edu

A.

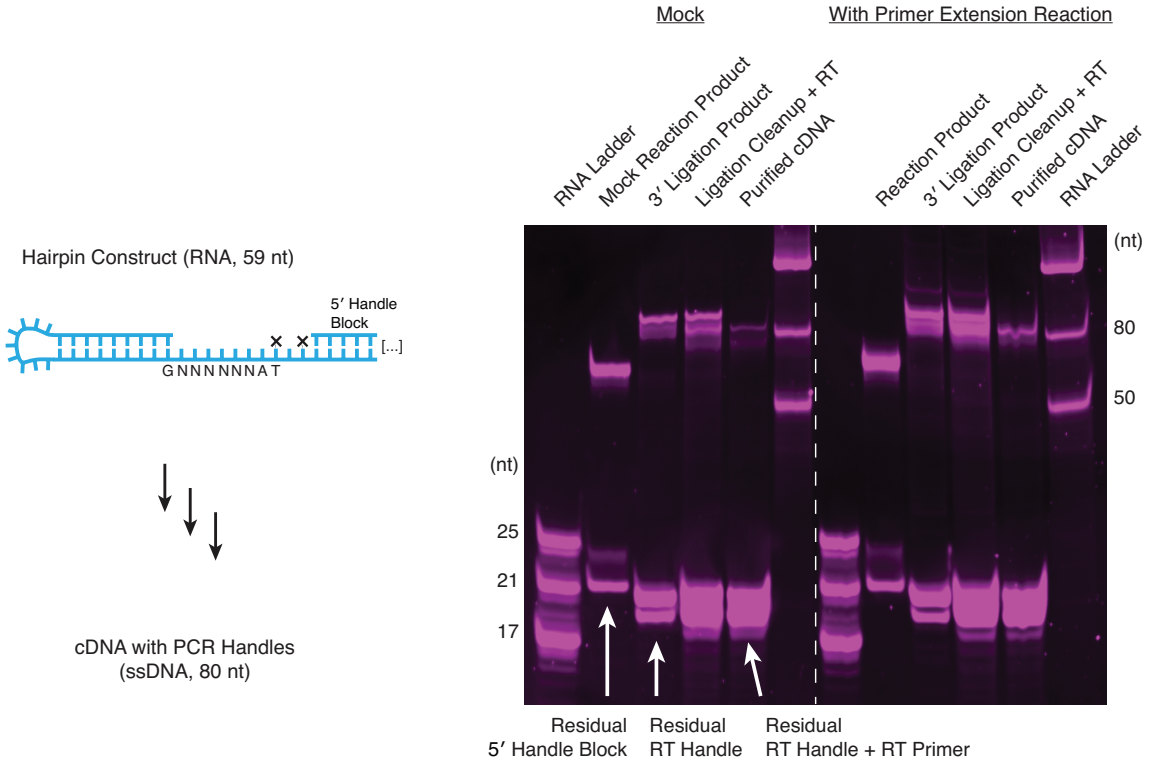

B.

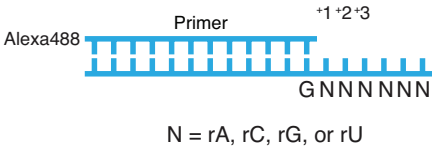

N = rA, rC, rG, or rU

C.

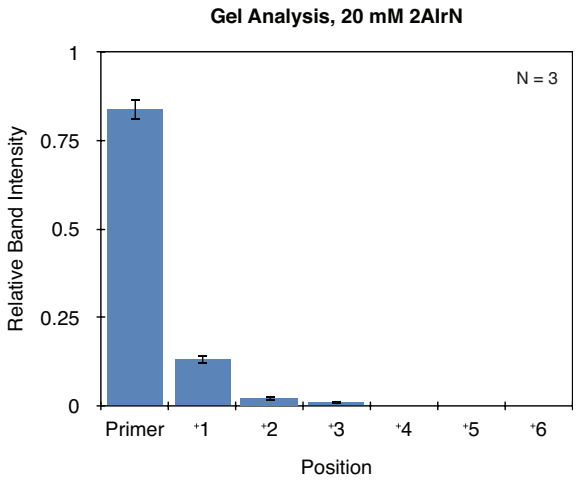

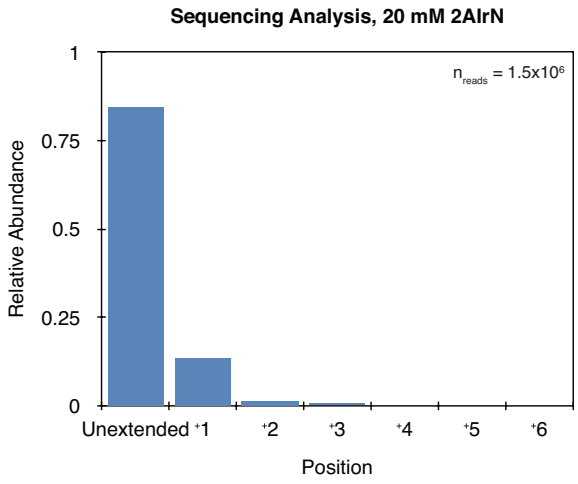

Figure S1. Validation of the Sequencing Assay with a Random-template Hairpin Construct and all Four Activated Nucleotides. A. Prior to deep-sequencing, the RT Handle (the template for the reverse transcription primer) is ligated to the 3′ terminus of the RNA hairpin construct, which is then reverse transcribed (RT). Denaturing polyacrylamide gel electrophoresis (PAGE) was used to visualize the efficiencies of RT Handle ligation and reverse transcription. The Mock condition ommitted activated nucleotides. Experimental conditions, in which the RNA hairpin was incubated with activated nucleotides for 24 hours, yield the same distribution of ligation and RT products as the Mock. This shows that there are no biases in the 3′ ligation of the RT Handle due to variable sequence ends. **B-C.** To validate the entire sequencing protocol, we compared the products of primer extension on a random template with all four activated nucleotides as measured by PAGE (N = number of PAGE experiments) to the equivalent reaction as measured by Nonenzymatic RNA Primer Extension Sequencing (NERPE-Seq) (n_{reads} = number of sequencing read pairs). The histograms show the distribution of product lengths in each case and are in excellent agreement. This demonstrates that NERPE-Seq does not introduce biases due to sequence variability or mismatches during sample preparation or data analysis (1). Experimental conditions for **B**: 5 µM 6N Template, 1 µM Control Primer, 200 mM Na^+ bicine, pH 8, and water were heated to 85°C for 30 s, then cooled to 23°C at 0.2 °C/s; 20 mM 2AIrN and 50 mM $MgCl_2$ were added to initiate the reaction. All concentrations indicate final concentrations in a volume of 20 µl. 1 µl aliquots were quenched in 40 µl Urea Load Buffer (8.3 M urea [Sigma-Aldrich], 1.3x TBE buffer [from a 10x autoclaved stock], 75 µM bromophenol blue [Sigma-Aldrich, from a 7.5 mM stock in DMSO], 880 µM orange G [Sigma-Aldrich, from an 88 mM stock in DMSO], syringe-filtered), 5 µl of which was mixed with 1 µl of a 300 µM stock of Randomer Primer Extension Reverse Complement, heated to 95°C for 3 minutes then cooled to 25°C at 0.2 °C/s. 14 µl additional Urea Load Buffer was added and samples were subjected to denaturing PAGE at 5 W for 20 minutes, then 15 W for 1 hour. A control without activated nucleotides was included for comparison.

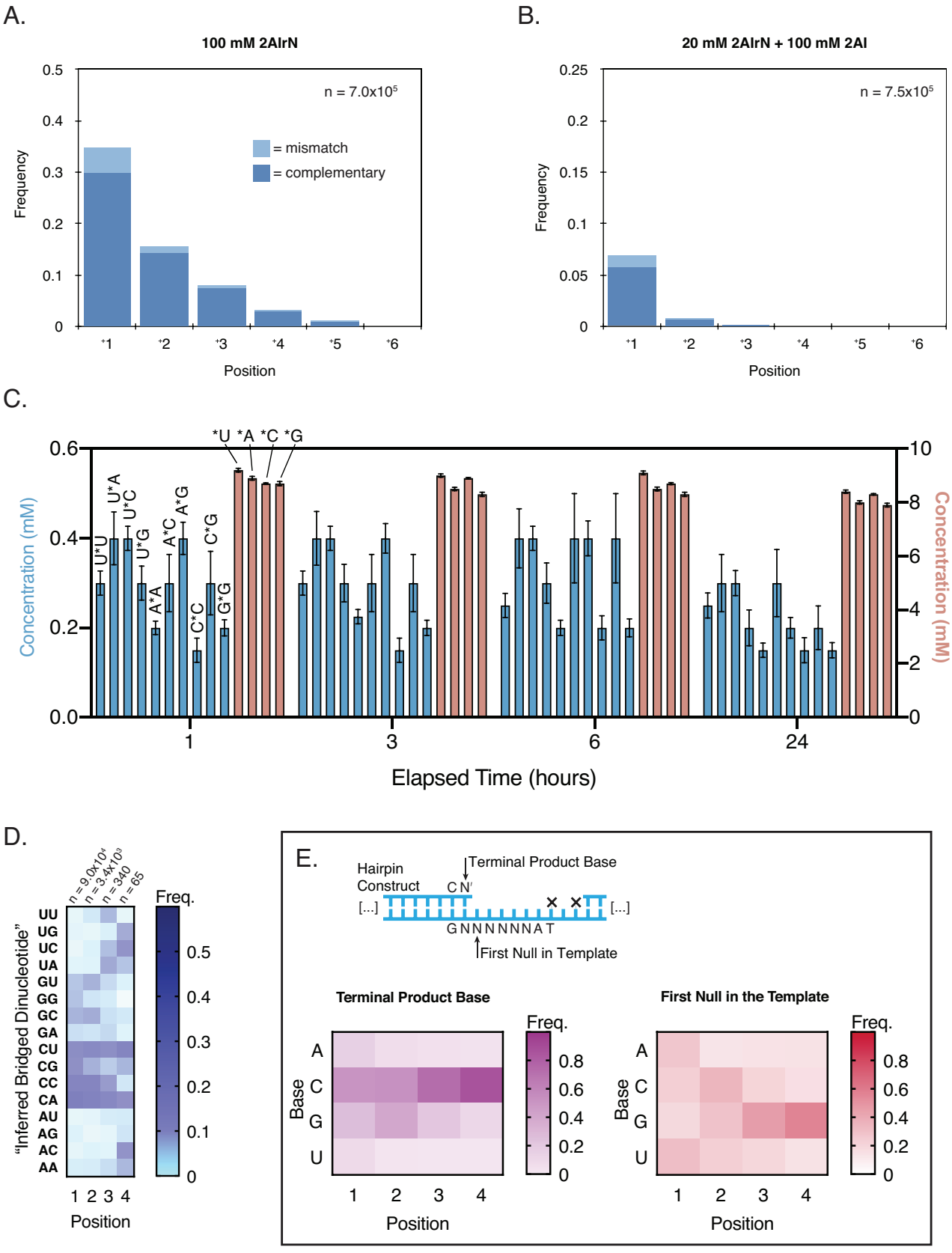
A.
100 mM 2AIrN
n = 7.0x10^5
= mismatch
= complementary
Frequency
Position
B.
20 mM 2AIrN + 100 mM 2AI
n = 7.5x10^5
Frequency
Position
C.
*U *A *C *G
U*U
U*A
U*C
U*G
A*A
A*C
A*G
C*C
C*G
G*G
Concentration (mM)
Concentration (mM)
Elapsed Time (hours)
D.
n = 9.0x10^4
n = 3.4x10^3
n = 340
n = 65
Freq.
"Inferred Bridged Dinucleotide"
UU
UG
UC
UA
GU
GG
GC
GA
CU
CG
CC
CA
AU
AG
AC
AA
Position
E.
Hairpin Construct
Terminal Product Base
GNNNNNNAT
First Null in Template
Terminal Product Base
First Null in the Template
Base
Freq.
Position

Figure S2. The Bridged Dinucleotide Intermediate Determines Complementary Product Sequences, Continued. A. Frequencies of complementary and mismatched nucleotide incorporations after 24 hours with 100 mM 2AIrN (compare with Figure 2A; n = unextended hairpins + total nucleotide incorporation events). **B.** Frequencies of complementary and mismatched nucleotide incorporations after 24 hours in the presence of 100 mM free 2AI, which inhibits accumulation of the bridged dinucleotide intermediate (compare with Figure 2A). **C.** Bridged dinucleotide (left axis scale) and activated mononucleotide (right axis scale) concentrations determined by NMR (see Material and methods for experimental details; ~10 mM starting concentration of each activated mononucleotide). Experimental error is high because the bridged dinucleotides accumulate to relatively low concentrations. Differences among many of the species are not significant, and the differences that are significant correlate with experimental error in the input concentrations of activated mononucleotides (*A and *U are at slightly higher concentrations than *C and *G). Furthermore, the differences do not correlate with inferred bridged dinucleotide frequencies. For example, C*C is measured as the lowest concentration bridged dinucleotide, but it is the most common inferred bridged dinucleotide (Figure 2D). We conclude that the concentrations of the various bridged dinucleotides are not responsible for the patterns of inferred bridged dinucleotides. ($MgCl_2$ had to be omitted from these experiments because magnesium-catalyzed hydrolysis reduces the bridged dinucleotide concentrations even further, making detection impossible.) **D.** "Inferred bridged dinucleotide analysis" of complementary products from a reaction with 50 mM OAtrN incubated for 24 hours. OAt-based primer extension cannot proceed through a bridged dinucleotide pathway; this analysis is a negative control for comparison with Figure 2D (P value = 0.0385 by Wilcoxon matched-pairs signed rank test). OAt-based primer extension is significantly less efficient than 2AI-based primer extension (see Figure S4D). Even with 50 mM reactants, very few products extend beyond +1 (note the low n-values at positions 3 and 4). **E.** Additional complementary product sequence features (data from the same experiment as in Figure 2). The distribution of terminal product bases is very similar to the overall product distribution (Figure 2B) because the majority of products of a given length are terminal (Figure S1C). The "first null in template" (see inset cartoon) distribution shows templating bases downstream of terminal product bases. There is a steady increase in rG in downstream positions because inferred bridged dinucleotides with a rC in the second position become progressively more frequent (Figure 2D).

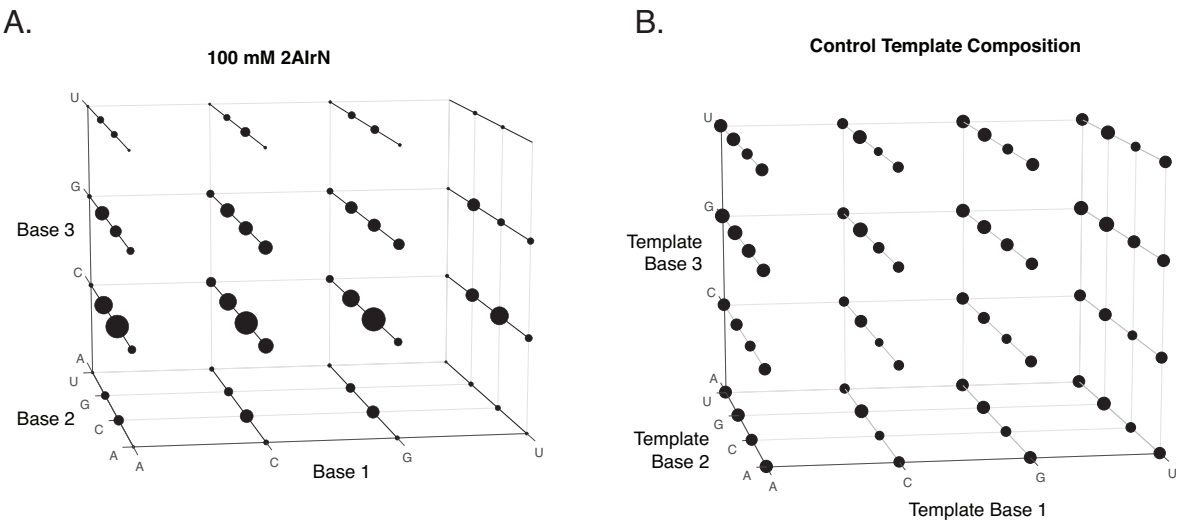

Figure S3. Complementary Product Sequence Space. A. The sequence space of primer extension with 100 mM 2AIrN, 24 hour incubation. The volume of each sphere is proportional to the frequency of each complementary product at least three bases long, beginning at position 1. **B.** The distribution of templating triplets in the random-template hairpin construct is relatively uniform. The data in Figure 3B and Figure S3A are not normalized because template composition biases (1) become smoothed out when considering longer stretches of templating bases. Supplemental Table 3 lists normalized data.

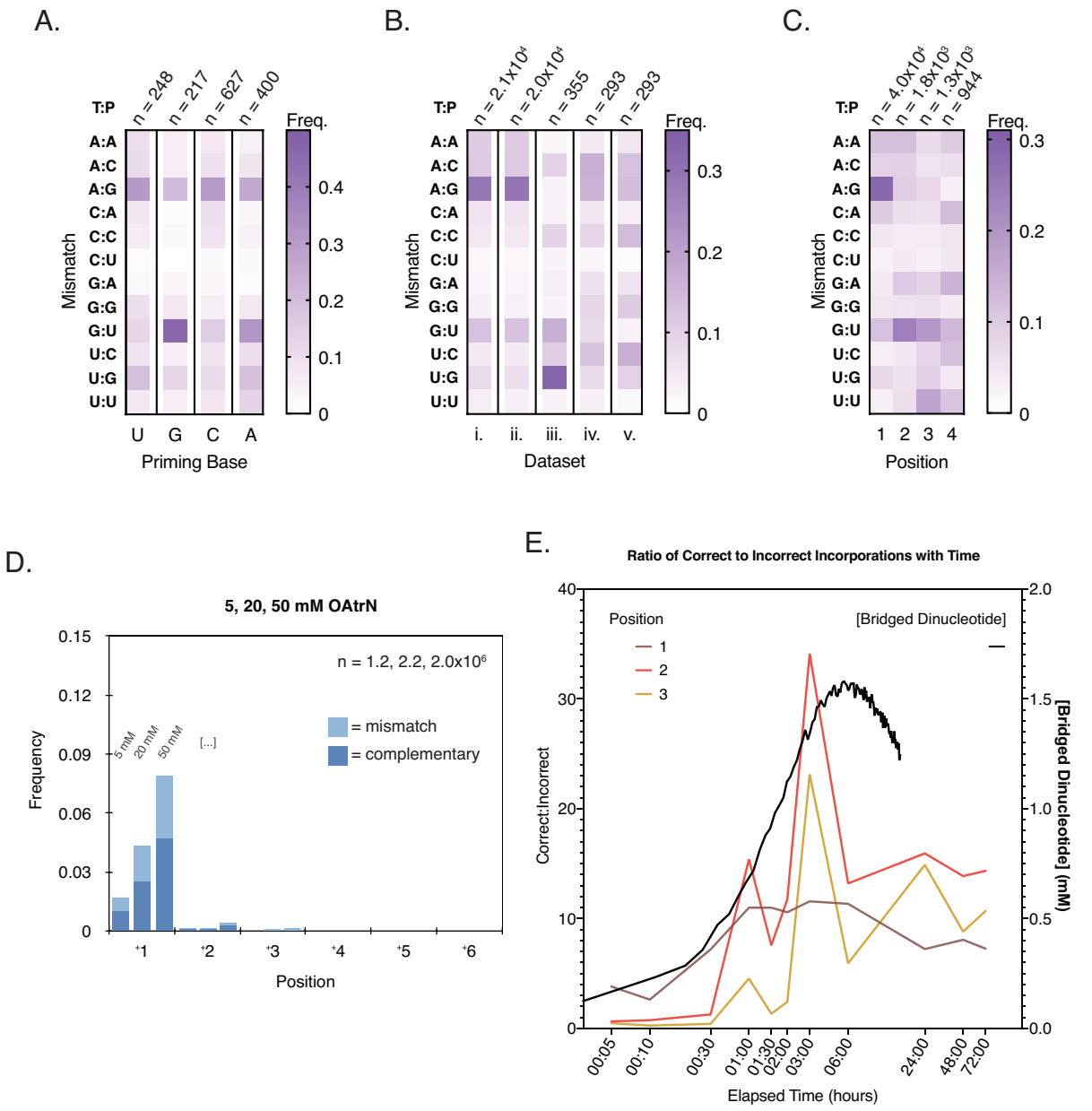

Figure S4. Mismatch Sequence Features. A. Mismatch frequencies at position 1 (20 mM 2AIrN, 24 hours; T:P = Template:Product), sorted by correctly paired priming base. This data is from an experiment with a hairpin construct that harbors all combinations of priming bases (rather than just rC, as in the primary construct [Figure 1A]). The distributions are similar except for the prevalence of G:U when the priming base is G. This combination of a GU wobble base pair adjacent to a correct base pair has been measured as the most energetically stable (2,3). (The same work also found that the G:U mismatch is always more stable than the U:G mismatch for each possible adjacent correct base pair. This explains why the frequency of G:U tends to be higher than that of U:G [Figure 4A]). **B.** Mismatch frequencies at position 1 (20 mM 2AIrN, 24 hours; T:P = Template:Product), sorted by features of adjacent positions. i. Position 1 mismatches (for comparison; same data as in Figure 4A). ii. Mismatches that are terminal. The majority of mismatches are terminal, so the distribution is the same as in (i.). iii. Mismatches that are followed by a correct incorporation. rC as the product base is favored because most of the subsequent

correct incorporations are rC or rG (44% C, 38% G, 13% A, and 5.5% U), and adjacent combinations of rC and rG are energetically stable (Figure 3A). Furthermore, the inferred bridged dinucleotides that drive a correct incorporation after a mismatch skew to rC in their second positions (48% C, 19% G, 18% A, and 15% U; n = 355). G:U and U:G mismatches are probably favored because they are the most energentically similar to a correct base pair (2-4). iv.-v. Mismatches that are followed by a mismatch, and mismatches that follow a mismatch. These distributions both exhibit low frequenices of product rA and especially rU, suggesting that base stacking is important for tandem mismatch formation (5). **C.** Position-dependent mismatch frequencies with OAt-activated mononucleotides (20 mM OAtrN, 24 hours). Compare with Figure 4A. The prominant G:U "streak" found with 2AI activation is missing because without the bridged dinucleotide pathway there is no enrichment among extended products for downstream templating rG. **D.** Frequencies of complementary and mismatched nucleotide incorporations at increasing concentrations of OAtrN after 24 hours. The overall mismatch frequency is comparable across the OAtrN concentrations, equaling 50.0%, 44.2%, and 43.2% for 5, 20, and 50 mM OAtrN, respectively. The low yields of +2 products are probably a consequence of the very high frequencies of mismatches at +1 position, which extend much less efficiently. (n = unextended hairpins + total nucleotide incorporation events.) **E.** Changes with time in the ratio of correct to incorrect incorporations (left axis) correlate with the formation of bridged dinucleotide over several hours and its subsequent hydrolysis (right axis) (6,7). The more pronounced spike in the ratio at positions 2 and 3 results from the more reactive G- and C-harboring bridged dinucleotides (Figure 2D) taking advantage of the G- and C-enriched templates selected at positions 2 and 3 by bridged dinucleotides reacting at upstream positions (Figure 3C-D). The minor peaks at the 1 and 24 hour timepoints may result from the high reaction frequency of rC-rich bridged dinucleotides when the overall concentration of bridged dinucleotides is relatively low (Figure 3D), either because they are still accumulating (at 1 hour) or because they have largely hydrolyzed (24 hours). The effect is most prominent at positions 2 and 3 because those templating positions (for templates with products that have already extended to +1 or +2) are enriched for rG (Figure 2B-D). The bridged dinucleotide data is from reference (7) and shows the concentration of A*A measured by ^{31}P NMR over 15 hours (10 mM 2AIrN, 200 mM HEPES, pH 8). The $MgCl_2$ concentration in that experiment was 30 mM instead of the 50 mM used in the reported sequencing experiments, so the bridged dinucleotide is expected to hydrolyze more slowly. This probably explains why the bridged dinucleotide concentration peak is slightly shifted to the right relative to the correct:incorrect incorporation ratio peaks.

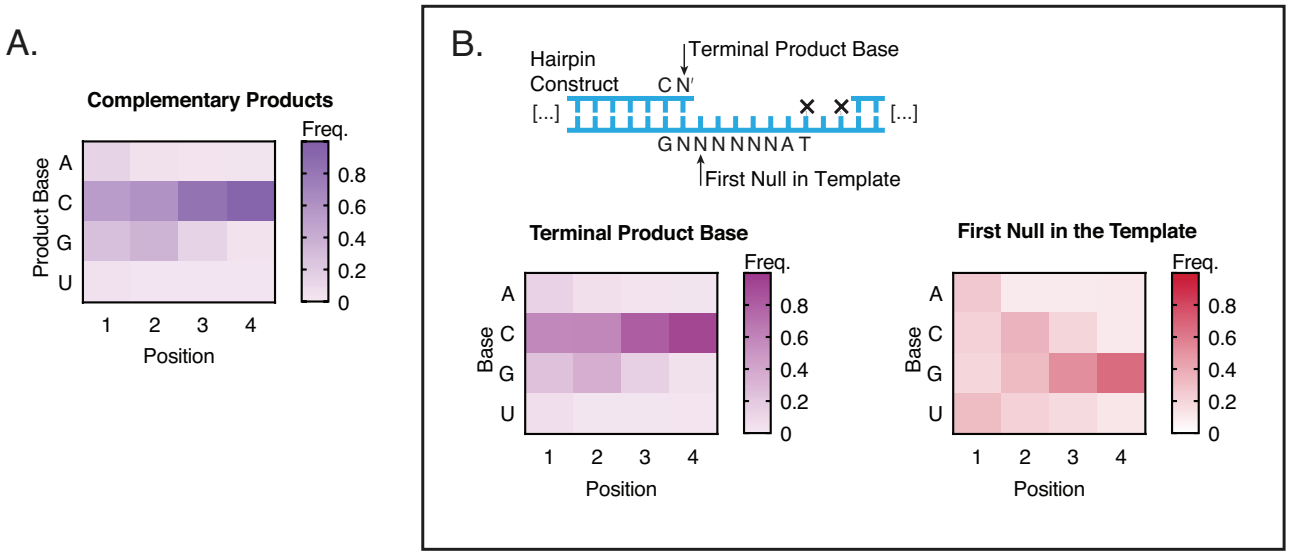

Figure S5. Complementary Product Sequence Features with Prebiotically Plausible Bridge-forming Activation Chemistry. A. Position-dependent base frequencies of complementary products for the same reaction as in Figure 5 (10 mM 2AIrN + MeNC-mediated bridge-forming activation, 24 hours). Compare to Figure 2B. **B.** Terminal product and first null in template distributions among complementary products for the same reaction as in Figure 5. Compare to Figure S2E.

Supplemental Table 1, Oligonucleotides

Oligo Name	Type	Source	Sequence (5′-3′; all termini free -OH unless otherwise noted)	Notes
Control Primer	RNA	IDT†	Alexa488-AGUGAGUAACUC	Figure S1
6N Template	RNA	In-house	NNNNNNGAGUUACUCACU	Figure S1
Randomer Primer Extension RC‡	RNA	In-house	AGUGAGUAACUCNNNNNN	Figure S1
6N	RNA/DNA	In-house	GUUCAGAGUUCUACAGUCCGACGAUCdT(-NPOM)CdT(-NPOM)ANNNNNNGCAUGCGACUAAACGUCGCAUGC	Random-template sequencing hairpin construct
MM	RNA/DNA	In-house	GUUCAGAGUUCUACAGUCCGACGAUCdT(-NPOM)CdT(-NPOM)ANNNNNNGCAUGCGACUAAACGUCGCAUGCN	Random-template sequencing hairpin construct with all possible priming base pair combinations; Figure S4A
5′ Handle Block	RNA	IDT	GUCGGACUGUAGAACUCUGAA-dideoxyC	
RT Handle	DNA	IDT	App-AGATCGGAAGAGCACACGTCT-dideoxyC	Template for the RT Primer
RT Primer	DNA	IDT	AGACGTGTGCTCTTCCGATCT	
PCR Primer 1 (NEBNext SR Primer for Illumina)	DNA	NEB	AATGATACGGCGACCACCGAGATCTACACGTTCAGAGTTCTACAGTCCG-s-A	
PCR Primer 2 (NEBNext Index Primer for Illumina)	DNA	NEB	CAAGCAGAAGACGGCATACGAGAT(6-base index)GTGACTGGAGTTCAGACGTGTGCTCTTCCGATC-s-T	

† IDT oligos ordered as RNase-free HPLC-purified
‡ RC = Reverse Complement, as competitor during PAGE analysis
⊥ See Material and Methods and (1) for details on in-house oligo synthesis and purification
App = riboA 5′-adenylation
dT(-NPOM) = NPOM-caged deoxyT (8)
N = rA, rU, rC or rG
-s- = thiol backbone linkage to inhibit exonucleases

Supplemental Table 2, Sequencing Experiments

Identifier	Expanded Identifier	Conditions	Notes
6N13	6N hairpin construct, 1 day, #3	200 mM Na^+ bicine, pH 8, 50 mM $MgCl_2$, 20 mM 2AIrN, 24 hour incubation	Figure S1
6NC4	6N hairpin construct, Control, #4	200 mM Na^+ bicine, pH 8, 50 mM $MgCl_2$, 24 hour incubation	Figure S1; used as the control for 6N13
6N1	6N hairpin construct, 1 day	200 mM Na^+ bicine, pH 8, 50 mM $MgCl_2$, 20 mM 2AIrN, 24 hour incubation	Primary experiment
6NC	6N hairpin construct, Control	200 mM Na^+ bicine, pH 8, 50 mM $MgCl_2$, 24 hour incubation	Used as the control for all 6N experiments except 6N13
6NXmin	6N hairpin construct, X = 5, 10, 30, 60, 90, 120, 180, and 360	200 mM Na^+ bicine, pH 8, 50 mM $MgCl_2$, 20 mM 2AIrN, 5-360 minute incubations	Figure 3C-D, Figure S4E
6N2 and 6N3	6N hairpin construct, 2 and 3 day	200 mM Na^+ bicine, pH 8, 50 mM $MgCl_2$, 20 mM 2AIrN, 48 and 72 hour incubations	Figure 3C-D, Figure S4E
6N100 or 6N [100]	6N hairpin construct, 100 mM 2AIrN	200 mM Na^+ bicine, pH 8, 50 mM $MgCl_2$, 100 mM 2AIrN, 24 hour incubation	Figure 3C-D, Figure S3A
6NXOAt	6N hairpin construct, X = 5, 20, and 50 mM OAtrN	200 mM Na^+ bicine, pH 8.9, 50 mM $MgCl_2$, 5-50 mM OAtrN, 24 hour incubation	Primer extension with OAt reactant activation requires a higher pH than that with 2AI activation (9), Figure 4, Figure S2D, Figure S4C-D
6N2AI	6N hairpin construct, free 2AI added	200 mM Na^+ bicine, pH 8, 50 mM $MgCl_2$, 20 mM 2AIrN, 100 mM 2AI (pH of stock adjusted to 8), 24 hour incubation	Figure 4, Figure S2B
MM20	MM hairpin construct, 20 mM 2AIrN	200 mM Na^+ bicine, pH 8, 50 mM $MgCl_2$, 20 mM 2AIrN, 24 hour incubation	Figure S4A
MMC	MM hairpin construct, Control	200 mM Na^+ bicine, pH 8, 50 mM $MgCl_2$, 24 hour incubation	Used as the control for MM20
6NDi60 and 180	6N hairpin construct, Dinucleotides, 60 and 180 minutes	200 mM Na^+ bicine, pH 8, 50 mM $MgCl_2$, 2 mM each bridged dinucleotide, 60 and 180 minute incubations	Purified bridged dinucleotides as reactants
6NMeNCId or 6NId	6N hairpin construct, MeNC-based bridge-forming activation, ideal conditions	200 mM HEPES, pH 8, 200 mM methyl isocyanide, 200 mM 2-methylbutyraldehyde, 20 mM 2AIrN, 30 mM $MgCl_2$, 24 hour incubation	Figure 5, Figure S5

Supplemental Table 3
Raw Counts of Each Sequence Triplet from the NERPE-Seq Analysis

Sequence Triplet	Figure 3B	Figure 3B, Template Normalized	Figure S3A	Figure S3A, Template Normalized
AAA	1	0.98	15	14.68
AAC	28	18.51	277	183.15
AAG	18	21.27	222	262.29
AAU	2	1.97	12	11.83
ACA	50	33.99	670	455.52
ACC	1746	947.61	6548	3553.81
ACG	79	70.57	1024	914.79
ACU	39	28.53	349	255.30
AGA	41	89.02	336	729.56
AGC	536	485.89	3096	2806.53
AGG	254	561.65	1743	3854.19
AGU	35	60.88	282	490.55
AUA	3	3.02	12	12.07
AUC	21	19.12	89	81.02
AUG	7	8.05	54	62.10
AUU	2	2.14	2	2.14
CAA	4	3.12	83	64.78
CAC	313	232.84	1816	1350.92
CAG	161	166.55	1494	1545.54
CAU	12	11.59	66	63.75
CCA	211	150.94	1356	970.03
CCC	2196	1521.94	6738	4669.79
CCG	231	264.09	1774	2028.16
CCU	111	92.82	759	634.71
CGA	20	31.45	373	586.47
CGC	612	543.16	2776	2463.73
CGG	379	791.48	1583	3305.83
CGU	22	36.29	252	415.74
CUA	14	12.17	88	76.51
CUC	72	73.51	548	559.52
CUG	14	16.19	266	307.59
CUU	1	0.93	20	18.58
GAA	1	1.52	45	68.31
GAC	29	33.80	308	359.02
GAG	72	139.66	796	1544.05
GAU	5	9.73	37	71.99
GCA	109	78.43	1163	836.80
GCC	1904	1107.09	7115	4137.05
GCG	135	129.85	1458	1402.34
GCU	72	52.85	595	436.78
GGA	41	128.59	473	1483.51

GGC	**543**	**701.12**	**2841**	**3668.27**
GGG	**221**	**763.94**	**1249**	**4317.45**
GGU	**49**	**118.98**	**316**	**767.30**
GUA	**5**	**7.28**	**41**	**59.73**
GUC	**47**	**64.87**	**275**	**379.57**
GUG	**11**	**19.61**	**147**	**262.07**
GUU	**28**	**38.30**	**58**	**79.34**
UAA	**0**	**0.00**	**15**	**12.28**
UAC	**40**	**24.08**	**237**	**142.67**
UAG	**13**	**13.00**	**169**	**168.97**
UAU	**0**	**0.00**	**3**	**2.75**
UCA	**7**	**5.26**	**138**	**103.66**
UCC	**1058**	**619.49**	**3239**	**1896.52**
UCG	**24**	**26.00**	**305**	**330.44**
UCU	**39**	**31.94**	**110**	**90.10**
UGA	**5**	**7.27**	**65**	**94.56**
UGC	**155**	**111.67**	**1207**	**869.55**
UGG	**130**	**206.30**	**1062**	**1685.31**
UGU	**7**	**8.02**	**76**	**87.12**
UUA	**0**	**0.00**	**3**	**2.71**
UUC	**19**	**14.73**	**42**	**32.57**
UUG	**0**	**0.00**	**16**	**16.24**
UUU	**0**	**0.00**	**3**	**2.52**

Numerical Data Used to Generate each Heat-map Figure

Figure 2B

A	**0.161**	**0.060**	**0.039**	**0.026**
C	**0.482**	**0.529**	**0.740**	**0.866**
G	**0.279**	**0.395**	**0.207**	**0.097**
U	**0.077**	**0.016**	**0.014**	**0.011**
	1	**2**	**3**	**4**

Figure 2D

U*U	**0.004998**	**0.001049**	**0.000955**	**0.000556**
U*G	**0.029812**	**0.004021**	**0.001623**	**0.000679**
U*C	**0.032706**	**0.009585**	**0.010638**	**0.008816**
U*A	**0.011283**	**0.002273**	**0.001858**	**0.001086**
G*U	**0.032555**	**0.070133**	**0.061527**	**0.033267**
G*G	**0.099501**	**0.147142**	**0.070761**	**0.047224**
G*C	**0.092312**	**0.145005**	**0.064933**	**0.021964**
G*A	**0.040646**	**0.039765**	**0.027148**	**0.01814**
C*U	**0.056508**	**0.046369**	**0.061829**	**0.069822**
C*G	**0.148704**	**0.074235**	**0.087508**	**0.147158**
C*C	**0.164694**	**0.303114**	**0.492484**	**0.519812**
C*A	**0.112924**	**0.093359**	**0.080057**	**0.105122**
A*U	**0.006954**	**0.001966**	**0.00175**	**0.002921**
A*G	**0.091019**	**0.031064**	**0.010785**	**0.007588**
A*C	**0.057323**	**0.025261**	**0.022484**	**0.012432**
A*A	**0.018061**	**0.005659**	**0.003661**	**0.003413**
	1	**2**	**3**	**4**

Figure 4A

A:A	**0.1077**	**0.0313**	**0.0554**	**0.0765**
A:C	**0.1130**	**0.0579**	**0.0614**	**0.0725**
A:G	**0.2909**	**0.1102**	**0.0853**	**0.0604**
C:A	**0.0608**	**0.0902**	**0.0495**	**0.0522**
C:C	**0.0512**	**0.1093**	**0.0879**	**0.0731**
C:U	**0.0215**	**0.0282**	**0.0220**	**0.0418**
G:A	**0.0272**	**0.0508**	**0.0763**	**0.1211**
G:G	**0.0344**	**0.0729**	**0.0940**	**0.0650**
G:U	**0.1298**	**0.2338**	**0.2454**	**0.2333**
U:C	**0.0470**	**0.0786**	**0.1021**	**0.1057**
U:G	**0.0764**	**0.0879**	**0.0676**	**0.0474**
U:U	**0.0400**	**0.0489**	**0.0532**	**0.0510**
	1	**2**	**3**	**4**

Figure 5B

U*U	**0.002458**	**0.001700**	**0.004564**	**0.007918**
U*G	**0.018179**	**0.002445**	**0.000000**	**0.001936**
U*C	**0.025494**	**0.005554**	**0.004387**	**0.001477**
U*A	**0.006213**	**0.001924**	**0.003700**	**0.007733**
G*U	**0.019668**	**0.043743**	**0.033430**	**0.010531**
G*G	**0.107418**	**0.134605**	**0.047332**	**0.008409**
G*C	**0.103310**	**0.146390**	**0.049600**	**0.012747**
G*A	**0.028856**	**0.029031**	**0.020144**	**0.009397**
C*U	**0.049552**	**0.036542**	**0.051641**	**0.083575**
C*G	**0.161059**	**0.071288**	**0.060481**	**0.098127**
C*C	**0.213329**	**0.398015**	**0.600000**	**0.600000**
C*A	**0.112262**	**0.081232**	**0.068740**	**0.074589**
A*U	**0.003854**	**0.002195**	**0.001858**	**0.001665**
A*G	**0.081448**	**0.023560**	**0.005250**	**0.001965**
A*C	**0.052740**	**0.018899**	**0.014571**	**0.013282**
A*A	**0.014159**	**0.002876**	**0.003535**	**0.001389**
	1	**2**	**3**	**4**

Figure 5C

A:A	0.0960	0.0593	0.0647	0.0679
A:C	0.0921	0.0663	0.0593	0.0719
A:G	0.2224	0.0681	0.0701	0.0519
C:A	0.0691	0.0763	0.0693	0.1088
C:C	0.0556	0.0910	0.0297	0.0466
C:U	0.0269	0.0566	0.0495	0.0466
G:A	0.0402	0.0820	0.0877	0.1259
G:G	0.0538	0.0621	0.0558	0.0498
G:U	0.1862	0.2436	0.2830	0.1669
U:C	0.0606	0.0804	0.0622	0.0975
U:G	0.0693	0.0659	0.0700	0.0686
U:U	0.0278	0.0482	0.0985	0.0975
	1	2	3	4

Figure S2D

UU	0.018066	0.039743	0.076732	0.017593
UG	0.020499	0.017394	0.031610	0.086030
UC	0.014315	0.029217	0.073746	0.098489
UA	0.023301	0.025531	0.087087	0.068733
GU	0.067223	0.081561	0.052391	0.029250
GG	0.070120	0.043313	0.036169	0.000000
GC	0.079886	0.085364	0.047649	0.038624
GA	0.047773	0.044577	0.054783	0.026100
CU	0.118651	0.137808	0.112911	0.156932
CG	0.109397	0.082404	0.063548	0.079286
CC	0.149406	0.151782	0.094752	0.040778
CA	0.183728	0.164051	0.139939	0.101991
AU	0.016627	0.020444	0.035148	0.036986
AG	0.028173	0.014692	0.020060	0.043671
AC	0.019004	0.027041	0.022965	0.098376
AA	0.033831	0.035077	0.050511	0.077160
	1	2	3	4

Figure S2E, Terminal Product Base

A	**0.153**	**0.062**	**0.043**	**0.027**
C	**0.508**	**0.528**	**0.725**	**0.859**
G	**0.256**	**0.393**	**0.216**	**0.103**
U	**0.082**	**0.017**	**0.015**	**0.011**
	1	**2**	**3**	**4**

Figure S2E, First Null in the Template

A	**0.275**	**0.128**	**0.139**	**0.144**
C	**0.234**	**0.348**	**0.211**	**0.154**
G	**0.186**	**0.289**	**0.455**	**0.560**
U	**0.305**	**0.234**	**0.195**	**0.142**
	1	**2**	**3**	**4**

Figure S4A

A:A	**0.1027**	**0.0592**	**0.0722**	**0.0455**
A:C	**0.1074**	**0.0592**	**0.0884**	**0.0812**
A:G	**0.3082**	**0.2039**	**0.3049**	**0.2598**
C:A	**0.0756**	**0.0194**	**0.1009**	**0.0335**
C:C	**0.0619**	**0.0290**	**0.0850**	**0.0430**
C:U	**0.0137**	**0.0000**	**0.0266**	**0.0239**
G:A	**0.0240**	**0.0338**	**0.0340**	**0.0185**
G:G	**0.1012**	**0.0713**	**0.0576**	**0.0723**
G:U	**0.1252**	**0.4652**	**0.1493**	**0.3187**
U:C	**0.0802**	**0.0592**	**0.0812**	**0.1036**
U:G	**0.1909**	**0.1237**	**0.1092**	**0.1886**
U:U	**0.0725**	**0.0538**	**0.0738**	**0.1328**
	U	**G**	**C**	**A**

Figure S4B

A:A	**0.1077**	**0.1099**	**0.0225**	**0.0494**	**0.0537**
A:C	**0.1130**	**0.1125**	**0.0951**	**0.1666**	**0.1289**
A:G	**0.2909**	**0.2977**	**0.0325**	**0.1574**	**0.1397**
C:A	**0.0608**	**0.0615**	**0.0292**	**0.0540**	**0.0404**
C:C	**0.0512**	**0.0498**	**0.0912**	**0.0900**	**0.1414**
C:U	**0.0215**	**0.0214**	**0.0292**	**0.0225**	**0.0101**
G:A	**0.0272**	**0.0266**	**0.0390**	**0.0618**	**0.0586**
G:G	**0.0344**	**0.0339**	**0.0278**	**0.0858**	**0.1071**
G:U	**0.1298**	**0.1301**	**0.1697**	**0.0755**	**0.0331**
U:C	**0.0470**	**0.0448**	**0.1043**	**0.1253**	**0.1716**
U:G	**0.0764**	**0.0717**	**0.3321**	**0.0745**	**0.0990**
U:U	**0.0400**	**0.0403**	**0.0274**	**0.0372**	**0.0165**
	i.	**ii.**	**iii.**	**iv.**	**v.**

Figure S4C

A:A	**0.1178**	**0.1189**	**0.0694**	**0.0974**
A:C	**0.0850**	**0.0885**	**0.0538**	**0.0614**
A:G	**0.2832**	**0.0943**	**0.0729**	**0.0313**
C:A	**0.0958**	**0.0619**	**0.0552**	**0.1248**
C:C	**0.0473**	**0.0373**	**0.0382**	**0.0481**
C:U	**0.0259**	**0.0428**	**0.0319**	**0.0466**
G:A	**0.0400**	**0.1012**	**0.0872**	**0.1436**
G:G	**0.0481**	**0.0520**	**0.0577**	**0.0408**
G:U	**0.1160**	**0.2387**	**0.1936**	**0.1334**
U:C	**0.0362**	**0.0458**	**0.0800**	**0.1185**
U:G	**0.0720**	**0.0560**	**0.0884**	**0.0451**
U:U	**0.0326**	**0.0625**	**0.1718**	**0.1090**
	1	**2**	**3**	**4**

Figure S5A

A	**0.140**	**0.043**	**0.025**	**0.019**
C	**0.531**	**0.597**	**0.826**	**0.927**
G	**0.278**	**0.349**	**0.138**	**0.038**
U	**0.051**	**0.011**	**0.012**	**0.017**
	1	**2**	**3**	**4**

Figure S5B, Terminal Product Base

A	**0.1350**	**0.0488**	**0.0259**	**0.0204**
C	**0.5780**	**0.5820**	**0.8090**	**0.9220**
G	**0.2340**	**0.3570**	**0.1540**	**0.0417**
U	**0.0531**	**0.0117**	**0.0114**	**0.0161**
	1	**2**	**3**	**4**

Figure S5B, First Null in Template

A	**0.2678**	**0.1022**	**0.1039**	**0.1090**
C	**0.2274**	**0.3572**	**0.2036**	**0.1084**
G	**0.1928**	**0.3185**	**0.5229**	**0.6595**
U	**0.3120**	**0.2221**	**0.1695**	**0.1232**
	1	**2**	**3**	**4**

SUPPLEMENTARY REFERENCES

1. Duzdevich, D., Carr, C.E. and Szostak, J.W. (2020) Deep sequencing of non-enzymatic RNA primer extension. *Nucleic Acids Res.*, **48**, e70.
2. Mathews, D.H., Sabina, J., Zuker, M. and Turner, D.H. (1999) Expanded sequence dependence of thermodynamic parameters improves prediction of RNA secondary structure. *Journal of Molecular Biology*, **288**, 911-940.
3. Turner, D.H. and Mathews, D.H. (2010) NNDB: the nearest neighbor parameter database for predicting stability of nucleic acid secondary structure. *Nucleic Acids Res.*, **38**, D280-D282.
4. Chen, J.L., Dishler, A.L., Kennedy, S.D., Yildirim, I., Liu, B., Turner, D.H. and Serra, M.J. (2012) Testing the Nearest Neighbor Model for Canonical RNA Base Pairs: Revision of GU Parameters. *Biochemistry*, **51**, 3508-3522.
5. Hayatshahi, H.S., Henriksen, N.M. and Cheatham, T.E. (2018) Consensus Conformations of Dinucleoside Monophosphates Described with Well-Converged Molecular Dynamics Simulations. *Journal of Chemical Theory and Computation*, **14**, 1456-1470.
6. Walton, T. and Szostak, J.W. (2017) A Kinetic Model of Nonenzymatic RNA Polymerization by Cytidine-5 '-phosphoro-2-aminoimidazolide. *Biochemistry*, **56**, 5739-5747.
7. Zhang, S.J., Duzdevich, D. and Szostak, J.W. (2020) Potentially Prebiotic Activation Chemistry Compatible with Nonenzymatic RNA Copying. *J. Am. Chem. Soc.*, **142**, 14810-14813.
8. Lusic, H. and Deiters, A. (2006) A new photocaging group for aromatic N-heterocycles. *Synthesis-Stuttgart*, 2147-2150.
9. Kervio, E., Sosson, M. and Richert, C. (2016) The effect of leaving groups on binding and reactivity in enzyme-free copying of DNA and RNA. *Nucleic Acids Res.*, **44**, 5504-5514.